THE ASTROPHYSICAL JOURNAL, 473:117–129, 1996 December 10

THE PUBLISHED EXTENDED ROTATION CURVES OF SPIRAL GALAXIES: CONFRONTATION WITH MODIFIED DYNAMICS

R. H. SANDERS
Kapteyn Astronomical Institute, Postbus 800, NL-9700 AV Groningen, The Netherlands; sanders@astro.rug.nl
Received 1996 April 29; accepted 1996 July 2

ABSTRACT

A sample of 22 spiral galaxy rotation curves, measured in the 21 cm line of neutral hydrogen, is considered in the context of Milgrom's modified dynamics (MOND). Combined with the previous, highly selected sample of Begeman et al., this constitutes the current total sample of galaxies with published (or available) extended rotation curves and photometric observations of the light distribution. This is the observational basis of present quantitative understanding of the discrepancy between the visible mass and classical dynamical mass in galaxies. It is found that the gravitational force calculated from the observed distribution of luminous material and gas by use of the simple MOND formula can account for the overall shape and amplitude of these 22 rotation curves, and in some cases, the predicted curve agrees with the observed rotation curve in detail. The fitted rotation curves have, in 13 cases, only one free parameter, which is the mass-to-light ratio of the luminous disk; in nine cases, there is an additional free parameter, which is M/L of a central bulge or light concentration. The values of the global M/L (bulge plus disk) are reasonable and, when the gas mass is also included, show a scatter consistent with that in the Tully-Fisher relation. The success of the MOND prescription in predicting the rotation curves in this larger, less stringently selected sample lends further support to the idea that dynamics or gravity is non-Newtonian in the limit of low acceleration and that it is unnecessary to invoke the presence of large quantities of unseen matter.

Subject headings: galaxies: kinematics and dynamics — galaxies: spiral — gravitation — radio lines: galaxies

1. INTRODUCTION

The conventional explanation for the discrepancy between the Newtonian dynamical mass and the luminous mass in galaxies is that the visible galaxy is embedded in a more extensive dark halo. But there are several unconventional explanations that involve modifications of the law of gravity or inertia (see Sanders 1990 for a review of the early suggestions). On a phenomenological level, the most successful of these suggestions is that of modified Newtonian dynamics (MOND) by Milgrom (1983). Here the central idea is that the law of gravity or inertia assumes a specific nonstandard form below a fixed, universal value of the acceleration, a_0, the one parameter of the theory (Milgrom 1983).

The rotation curves of spiral galaxies as measured in the 21 cm line of neutral hydrogen constitute the ideal body of data to confront such ideas. This is because the rotation curves usually extend well beyond the optical image of the galaxy, where the discrepancy is large, and because gas on very nearly circular orbits is the most precise probe of the radial force law in the limit of low acceleration. Rotation curves are not useful as tests of the dark matter hypothesis because models consisting of a luminous disk plus an extended dark halo generally have at least three adjustable parameters and can always be concocted to fit the rotation curves (Rhee 1996); by fitting to rotation curves, one simply determines the parameters of the assumed halo model. Although the plausibility of the fitted values of parameters is sometimes questionable, it is not possible to definitively falsify the dark matter hypothesis in this way. On the other hand, MOND, with only one universal parameter, which cannot vary from galaxy to galaxy, is far less flexible and far more falsifiable.

The essential problem with the use of such data for this purpose is that the measured rotation curves are not all equally good approximations to the run of circular velocity. In many galaxies, there are complications that arise from warping of the gas layer in the outer regions; this gives an intrinsic uncertainty to the inclination and position angle of the plane of the disk. In other galaxies, the observation of highly asymmetric gas disks calls into question the assumption of relaxed motion on circular orbits. Apart from the rotation curves, an additional problem is that, by whatever theory of gravity one applies, the radial force due to the detectable matter is calculated by assuming that the distribution of visible light is the precise tracer of matter in the stellar disk and that the distribution of neutral hydrogen is a tracer of the gaseous mass distribution. These assumptions can fail in several respects: for example, when there are radial color gradients in a galaxy, not all color bands can be equally good tracers of the visible mass distribution. With respect to the gaseous component, the radial distribution and even the normalization of the mass of molecular gas is unknown for most spiral galaxies.

With a view toward minimizing these problems, Begeman, Broeils, & Sanders (1991, hereafter BBS) applied strict selection criteria to the rotation curves available at the time ($\sim$20). Most of these criteria are relevant to the 21 cm line observations: the rotation curve had to be derived from two-dimensional, high spatial resolution data, which eliminates distant galaxies (systemic velocity greater than 2000 km s^{-1}); galaxies with highly warped or asymmetric gas disks and those with patchy H I distributions were not considered. High-precision photometric data (CCD, in general) had to be available for estimating the contribution of the visible disk to the radial force law.

A total sample of 11 galaxies met these criteria. The conclusion of the rotation-curve fitting was that MOND, with a fixed value for the acceleration parameter and with one free parameter per galaxy (M/L for the visible disk), worked as well as multiparameter dark halo models; in fact, with respect to fitting details of the rotation curves, MOND worked even better in several cases. The success of MOND in predicting the run of circular velocity in galaxies from the observed distribution of detectable matter is one of the strongest arguments in its favor. No simple prescription for reducing the number of dark halo parameters works as well as the MOND formula (see Sanders & Begeman 1994). At very least, the simple MOND formula provides the most efficient fitting algorithm for spiral galaxy rotation curves. This implies that, whatever its cause, the discrepancy between the Newtonian dynamical mass and the visible mass appears below a fixed, universal acceleration.

BBS could be, and have been, criticized for being too selective. One might ask to what extent criteria are applied, at least unconsciously, that eliminate those cases that contradict MOND. Partly to respond to such criticism and partly because the sample of galactic rotation curves available in the literature is now larger, it was decided to repeat the analysis of BBS for a less stringently selected sample. An additional 22 galaxies are considered here, the rotations curves of most of which are published or will soon be published. Because dark halo models have been presented elsewhere and because the experience is that multiparameter dark halo models can always fit rotation curves, the only comparison is with the rotation curve predicted by MOND, using the observed distribution of detectable matter insofar as it is traced by the visible light and the neutral hydrogen.

The essential result of this work is that MOND, with one free parameter per galaxy—in some cases two, if a bulge is present—accounts for the magnitude of the discrepancy and reproduces the general shape of the rotation curves of these 22 additional spiral galaxies. This is particularly striking when one keeps in mind the observational caveats mentioned above and considers that the galaxies in the present sample have asymptotic rotational velocities ranging from less than 60 km s^{-1} to 300 km s^{-1} and cover a range of 1000 in luminosity. In some individual cases the fits are remarkably good, comparable to the best fits in the highly selected BBS sample. The values of the fitted parameter, the luminous mass or the implied value of M/L, are reasonable in terms of population synthesis models and have a small scatter, particularly in the near-infrared. On the whole, the idea is given further support by comparison with this larger, less stringently selected sample of galactic rotation curves.

2. SAMPLE

The 22 galaxies considered here are listed in Table 1. These, combined with the 11 galaxies in BBS, constitute the current total sample of objects with well-measured 21 cm line rotation curves and accurate surface photometry in at least one color band. There is much overlap with similar lists given by Broeils (1992) and by Rhee (1996). Most of the rotation curves here were taken directly from the literature, but two have not yet been published (M33, NGC 1003) and were communicated privately.

This is a motley collection of galaxies observed either at the VLA or at Westerbork, with varying degrees of precision. The sample includes several very large and luminous galaxies such as UGC 2885 and NGC 801, originally made famous by Rubin et al. (1985) as examples of spiral galaxies

TABLE 1

SAMPLE GALAXIES IN ORDER OF DECREASING ROTATIONAL VELOCITY

Galaxy (1)	Type (2)	D (Mpc) (3)	L_B ($10^{10} L_\odot$) (4)	L_H ($10^{10} L_\odot$) (5)	$R_{H\,II}$ (kpc) (6)	M_{gas} ($10^{10} M_\odot$) (7)	V_{rot} (km s^{-1}) (8)	a (10^{-8} cm s^{-2}) (9)	References (10)
UGC 2885.....	Sbc	79	21	...	73	5.0	300	0.40	1, 2
NGC 5533.....	Sab	54	5.6	...	74	3.0	250	0.27	3, 4, 5
NGC 6674.....	SBb	49	6.8	...	69	3.9	242	0.28	3, 4
NGC 5907.....	Sc	11	2.4	4.9	32	1.1	214	0.46	6, 7
NGC 2998.....	SBc	67	9.0	...	47	3.0	213	0.31	3, 4
NGC 801	Sc	80	7.4	...	59	2.9	208	0.24	1, 3
NGC 5371.....	S(B)b	34	7.4	...	40	1.0	208	0.35	8, 9
NGC 5033.....	Sc	11.9	1.9	3.9	35	0.93	195	0.35	8, 10
NGC 3521.....	Sbc	8.9	2.4	...	28	0.63	175	0.35	10, 11
NGC 2683.....	Sb	5.1	0.6	...	18	0.05	155	0.43	10, 11
NGC 6946.....	SABcd	10.1	5.3	...	30	2.7	160	0.28	12
UGC 128	LSB[a]	56.4	0.52	...	40	0.91	130	0.14	13, 14
NGC 1003.....	Scd	11.8	1.5	0.45	33	0.82	110	0.12	3, 4
NGC 247	SBc	2.8	0.35	0.22	11	0.13	107	0.34	15, 16
M33	Sc	0.84	0.74	0.43	8.3	0.13	107	0.45	17, 18, 19
NGC 7793.....	Scd	3.1	0.34	0.17	6.7	0.096	100	0.48	16, 20
NGC 300	Sc	2.15	0.3	...	12.7	0.13	90	0.21	15, 16
NGC 5585.....	SBcd	7.6	0.24	0.14	12	0.25	90	0.22	21
NGC 2915.....	BCG[b]	5.6	0.036	...	15	0.1	90	0.17	22, 23
NGC 55	SBm	1.6	0.43	...	9	0.13	86	0.27	24
IC 2574	SBm	3.0	0.08	0.022	8	0.067	66	0.18	25
DDO 168.....	Irr	3.8	0.022	...	3.7	0.032	54	0.26	3

[a] Low surface brightness.

[b] Blue compact galaxy.

REFERENCES.—(1) Kent 1986; (2) Roelfsema & Allen 1985; (3) Broeils 1992; (4) Broeils & Knapen 1991; (5) Kent 1984; (6) Barnaby & Thronson 1992, 1994; (7) Sancisi & van Albada 1987; (8) Begeman 1987; (9) Wevers 1984; (10) Kent 1985; (11) Casertano & van Gorkom 1991; (12) Carignan et al. 1990; (13) van der Hulst et al. 1993; (14) de Blok et al. 1995; (15) Carignan & Puche 1990b; (16) Carignan 1985; (17) Deul & van der Hulst 1987; (18) Rhee 1996; (19) Kent 1987; (20) Carignan & Puche 1990a; (21) Coté, Carignan, & Sancisi 1991; (22) Meurer et al. 1994; (23) Meurer et al. 1996; (24) Puche, Carignan, & Wainscoat 1991; (25) Martimbeau & Carignan 1994.

with extended nondeclining rotation curves, as well as gas-dominated dwarfs such as IC 2574 and DDO 168 with gently rising rotation curves. There are two galaxies with distinctly declining rotation curves, NGC 2683 and NGC 3521, observed by Casertano & van Gorkom (1991), who emphasized this general trend in high surface brightness galaxies. There is one recently observed low surface brightness galaxy, UGC 128 (van der Hulst et al. 1993; de Blok, van der Hulst, & Bothun 1995), and one blue compact galaxy, NGC 2915 (Meurer, Mackie, & Carignan 1994; Meurer et al. 1996).

The columns in the table are generally self-explanatory. The objects are listed in order of decreasing asymptotic rotational velocity. The adopted distance (col. [3]) is of critical importance in MOND fits because the internal accelerations scale inversely as the distance. Indeed, as was demonstrated by BBS, the distance can be taken as a free parameter of the MOND fit. The Hubble law distance is taken for the more distant objects with $H_0 = 75$ km s^{-1} Mpc^{-1}, corrected for Local Group motion. Recently determined Cepheid distances were taken for M33 (Madore & Freedman 1991) and NGC 300 (Freedman et al. 1992). Distances to other nearby galaxies (e.g., the Sculptor Group galaxies) have been taken from the listed references. For several objects a correction for Virgocentric inflow was included, following Kraan-Korteweg (1986), but in general this did not differ from the straight Hubble law distance by more than 10%. The corrected blue luminosity (col. [4]) is taken from the primary references, and the near-infrared luminosity (col. [5]) is calculated from the H-band apparent magnitudes given by Tormen & Burstein (1995). The extent of the observed H I rotation curve is listed in column (6). The total gas mass, hydrogen plus helium, assuming that this is 1.3 times the measured H I mass, is given in column (7). The value of the rotational velocity at the outermost radius is given in column (8), and the corresponding centripetal acceleration in column (9). Column (10) gives the numbered references for the rotation curve and for the photometry.

Nine of the galaxies in this sample show clear evidence in the radial light distribution for a central bulge component; these are listed in Table 2. Because the bulge is generally assumed to have a more spheroidal shape and because one may wish to assign a separate mass-to-light ratio to the bulge component, a decomposition of the profile into bulge and disk components is necessary. The bulge-disk decomposition given in the indicated references is taken in the cases of NGC 5907, 3521, and 2683. In the cases of UGC 2885, NGC 801, and NGC 2998, the light distribution for the bulge is taken from the double-exponential decompositions (i.e., exponential bulge and disk) by Andredakis & Sanders (1994). Additional double-exponential decompositions were supplied for NGC 5533, 6674, and 5371 by Y. C. Andredakis (1996, private communication). In most of these cases of an exponential bulge fit, the radial distribution of disk light was determined by subtracting the smooth bulge profile from the total radial intensity profile (i.e., the disk light distribution is not assumed to be exponential but is that actually observed after subtraction of the bulge). The length scale (the exponential scale length or effective radius) and axial ratio of the bulge and bulge-to-total luminosity ratios are listed in columns (4) and (5) of Table 2.

TABLE 2

BULGE-DISK DECOMPOSITIONS

Galaxy (1)	Bulge Model (2)	r_b (kpc) (3)	b/a (4)	B/T (5)	Reference (6)
UGC 2885.....	Exponential	0.6	0.86	0.07	1, 2
NGC 5533.....	Exponential	1.7	1.00	0.42	3, 4
NGC 6674.....	Exponential	1.1	0.90	0.79	3, 4
NGC 5907.....	Hubble	0.2	0.45	0.17	5
NGC 2998.....	Exponential	1.0	0.49	0.10	1, 2
NGC 801	Exponential	1.1	0.75	0.35	1, 2
NGC 5371.....	Exponential	0.9	1.00	0.36	3, 6
NGC 3521.....	$r^{1/4}$	0.5	0.52	0.17	7
NGC 2683.....	$r^{1/4}$	1.7	0.21	0.30	7

REFERENCES.—(1) Kent 1985; (2) Andredakis & Sanders 1994; (3) Y. C. Andredakis 1996, private communication; (4) Broeils & Knapen 1991; (5) Barnaby & Thronson 1992, 1994; (6) Begeman 1987; (7) Kent 1985.

3. PROCEDURE

To calculate MOND rotation curves, the same procedure was followed as in BBS. The first step is to determine the Newtonian rotation curve of the detectable matter. This is done by assuming that the light in the disk is a precise tracer of the luminous matter (i.e., no radial variation of M/L in a given galaxy) and that this matter has an axisymmetric distribution in an infinitesimally thin disk. In those nine cases for which there is a bulge-disk decomposition, it is also assumed that the mean radial distribution of light in the bulge component traces its luminous mass distribution and, for simplicity of calculation, that the bulge mass distribution is spherically symmetric. These calculations were repeated assuming that the bulge was highly flattened (a disk), but in general there was no significant difference in the rotation-curve fit (although the fitted bulge mass is lower).

The gaseous mass distribution is assumed to be traced by the mean radial distribution of neutral hydrogen. The H I surface density is everywhere increased by a factor of 1.3 to account for the contribution of helium. This of course neglects any contribution of molecular gas, which, in the absence of more detailed information, is assumed to be distributed as the luminous component (Young 1987). The gas distribution is also taken to be axisymmetric in an infinitesimally thin disk.

Given the Newtonian acceleration, g_N, the true gravitational acceleration, g, is determined from the MOND formula

$$\mu(g/a_0)g = g_N , \tag{1}$$

where a_0 is the MOND acceleration parameter and

$$\mu(x) = x(1 + x^2)^{-1/2} . \tag{2}$$

This commonly assumed form has the appropriate asymptotic behavior, yielding Newtonian dynamics in the high-acceleration limit and MOND dynamics in the low-acceleration limit (Milgrom 1983). For several galaxies in the sample (e.g., IC 2574), $g \ll a_0$ everywhere, so the exact form of μ is unimportant. The rotation law is given, as usual, by

$$v^2/r = g , \tag{3}$$

which means that, with equations (1) and (2), as r becomes large,

$$v^4 = GM_t a_0 , \tag{4}$$

where M_t is the total finite mass of the galaxy in stars and gas ($M_t = M^* + M_g$). In the determination of g, it would be desirable to apply the physically consistent field equation of Bekenstein & Milgrom (1984), but this is computationally difficult. Moreover, it has been demonstrated that the simple MOND formula yields, in most cases, results that agree quite closely with the integration of the full field equation (Milgrom 1986; Brada & Milgrom 1995). In the context of inertia-modified theories of MOND (Milgrom 1994), equation (1) would be exact.

The observed rotation curve is fitted in a least-squares program by applying equations (1)–(3). The free parameter of the fit is always M_d, the total mass of the luminous disk, and, for those cases in Table 2, M_b, the mass of the bulge. In combination with the observed luminosities, this yields the mass-to-light ratio of the luminous components. The total stellar mass of a galaxy is $M^* = M_d + M_b$.

Here the acceleration parameter a_0 is not allowed to be free but is taken to be the mean value determined by the fits to the higher quality rotation curves of BBS, i.e., $1.2 \times 10^{-8}[H_0/(75 \text{ km s}^{-1} \text{ Mpc}^{-1})]$ cm s^{-2}. It is a questionable procedure, in principle, to take a quantity supposed to be a fundamental constant as a fitting parameter (Milgrom 1988). Moreover, unlike BBS, who fitted the rotation curves by allowing the distance to a galaxy to be both fixed and free, here we fix the distance at the adopted value given in Table 1. This is done because it is desirable to reduce the dimensionality of the parameter space when the data are less precise. Random or systematic errors in the estimated circular velocity at a few points can yield solutions in an extreme region of a multidimensional parameter space; i.e., minima in the χ^2-surface that appear to be sharp are, in fact, very broad as a result of underestimated errors in observed rotational velocity. In principle, this problem could be eliminated by a realistic estimate of the errors, but in practice this is very difficult when there are unknown systematic effects (e.g., warps, bars, pressure support, beam smearing). Therefore, with a_0 and distance fixed, the quality of the fit can be judged by visual inspection and the plausibility of the implied M/L-ratios.

4. RESULTS

The results are given in Figure 1 and in Table 3. In the figure, we see the observed rotation curve (*points with error bars*) compared with the fitted MOND rotation curve (*solid lines*). The Newtonian rotation curves of the various individual components are also shown.

A word is necessary about the indicated error bars. These are taken, in general, directly from the reference for the rotation curve (Table 1) and cannot be interpreted in a uniform way. Often the indicated errors are formal 1 σ errors returned by the program that fits tilted rings to the two-dimensional H I velocity field. These are unrealistically low because this technique does not include an assessment of the possible systematic effects. In other cases, error bars are estimated by performing the tilted-ring analysis separa-

TABLE 3

MOND Masses and Implied M/L-Values for the Total Sample

Galaxy (1)	M_d (10^{10} $M_\odot$) (2)	$(M/L)_d$ (3)	M_b (10^{10} $M_\odot$) (4)	$(M/L)_b$ (5)	M^*/L_B (6)	M_t/L_B (7)	M_t/L_H (8)
UGC 2885	25.1	1.3	5.7	3.9	1.5	1.7	...
NGC 2841[a]	24.1	3.5	6.9	4.3	3.7	4.0	1.9
NGC 5533	2.0	0.6	17.0	7.2	3.4	3.9	...
NGC 6674	2.5	1.8	15.5	2.9	2.6	3.2	...
NGC 7331[a]	8.6	3.8	4.7	1.5	2.5	2.7	0.8
NGC 5907	7.2	1.6	2.5	6.8	3.9	4.3	2.2
NGC 2998	5.4	0.9	2.9	4.3	1.2	1.7	...
NGC 801	3.5	0.7	6.5	2.5	1.4	1.7	...
NGC 5371	6.7	1.4	4.8	1.8	1.6	1.7	...
NGC 5033	8.8	4.6	...	...	4.6	5.1	2.5
NGC 2903[a]	5.5	3.6	...	...	3.6	3.8	2.7
NGC 3521	6.2	3.1	0.3	0.7	2.7	...	...
NGC 2683	3.0	6.4	0.5	2.8	5.8	...	...
NGC 3198[a]	2.3	2.6	...	...	2.6	3.3	3.6
NGC 6946	2.7	0.5	...	...	0.5	1.0	...
NGC 2403[a]	1.1	1.4	...	...	1.4	2.0	1.6
UGC 128	0.57	1.1	...	...	1.1	2.8	...
NGC 6503[a]	0.83	1.7	...	...	1.7	2.2	2.3
NGC 1003	0.30	0.2	...	...	0.2	0.7	2.5
NGC 247	0.40	1.1	...	...	1.1	1.5	2.3
M33	0.48	0.65	...	...	0.6	0.8	1.4
NGC 7793	0.41	1.20	...	...	1.2	1.5	2.8
NGC 300	0.22	0.73	...	...	0.7	1.2	...
NGC 5585	0.12	0.50	...	...	0.5	1.5	2.6
NGC 2915	0.25	6.9	...	...	6.9	9.7	...
UGC 2259[a]	0.22	2.1	...	...	2.1	2.6	...
NGC 55	0.10	0.23	...	...	0.2	0.5	...
NGC 1560[a]	0.034	1.0	...	...	1.0	3.8	2.1
IC 2574	0.01	0.13	...	...	0.1	1.0	3.5
DDO 170[a]	0.024	1.5	...	...	1.5	5.3	...
NGC 3109[a]	0.005	0.1	...	...	0.1	1.4	...
DDO 168	0.005	0.23	...	...	0.2	1.7	...
DDO 154[a]	0.004	0.11	...	...	0.1	9.1	...

[a] From the sample of BBS.

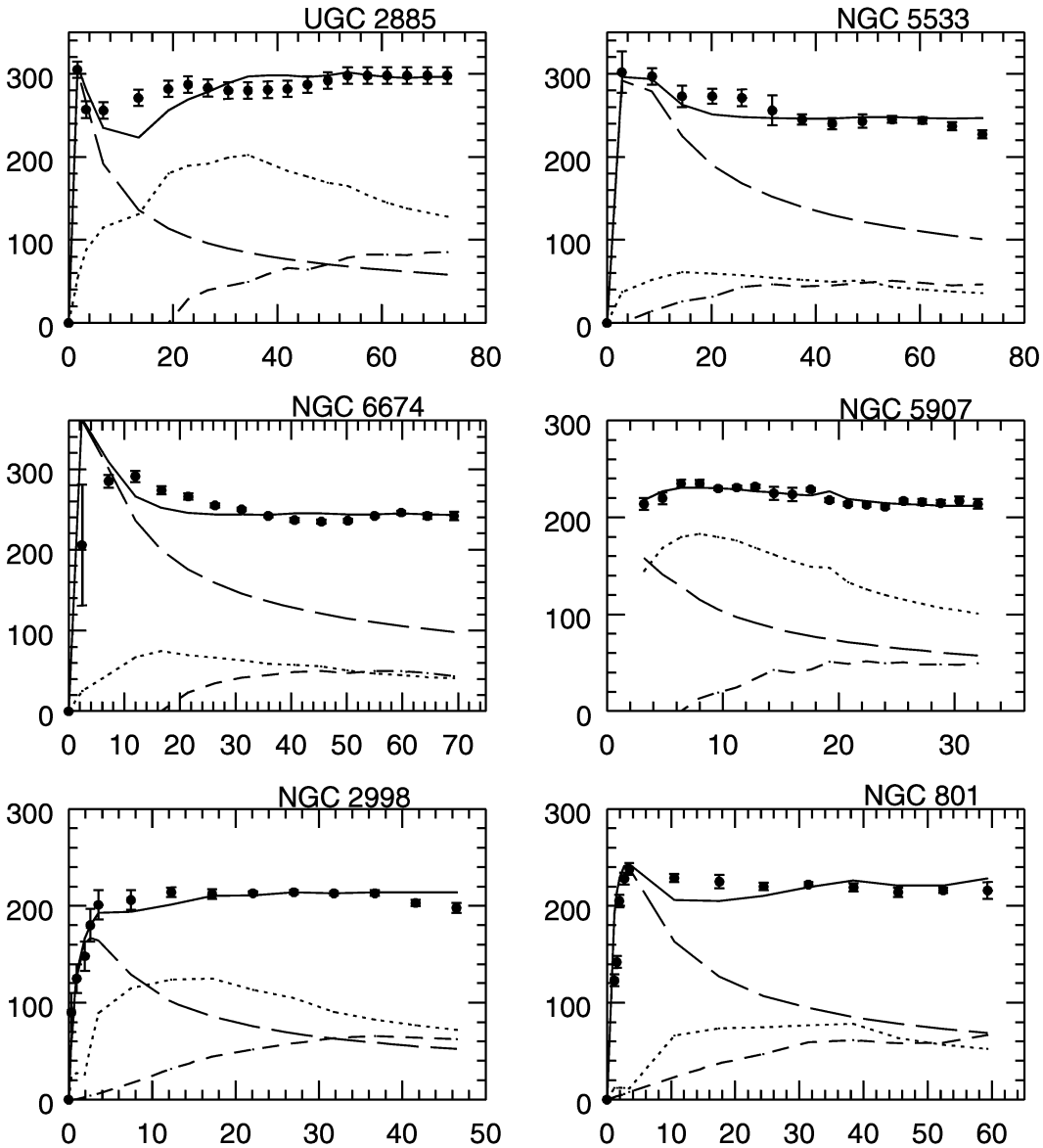

FIG. 1.—MOND fits to the rotation curves of the sample galaxies. The radius (*horizontal axis*) is in kpc in all cases, and the rotational velocity is in km s^{-1}. The points with error bars are the observations, and the solid line is the rotation curve determined from the distribution of light and neutral hydrogen with the MOND formula. The other lines are the Newtonian rotation curves of the various separate components: the long-dashed line is the rotational velocity resulting from a central bulge, if present; the short-dashed line is the rotation curve of the gas disk (H I plus He); the dotted line is that of the luminous disk. The free parameter(s) of the fitted curve are the disk mass and, if present, the bulge mass. The sample galaxies are shown in order of decreasing asymptotic circular velocity.

tely for two different sides of the galaxy (approaching and receding) and taking the difference between the resulting rotation curves. This yields a fairer assessment of those systematic errors that result from asymmetries in the velocity field. In any case, the commonly used tilted-ring algorithm is, at best, a first-order correction to the effects of warping in estimating the circular velocity.

The rotation curves are given as listed in Table 1, ordered by decreasing asymptotic rotational velocity. The first rotation curves are those of large luminous systems with bulges or, at least, central light concentrations. These are distant galaxies, so the spatial resolution of the 21 cm line observations is generally several kiloparsecs. The MOND fits indicate that the mass distribution in several of these galaxies is more centrally concentrated than the light distribution, implying that the bulges have a significantly higher M/L than the disk. The rotation curves in the last two panels are those of relatively nearby dwarfs. These are systems without bulges, in which the gas makes a significant contribution to the total Newtonian force in the outer regions. Several of these systems are irregular, with asymmetric velocity fields.

It is necessary to discuss several of the individual galaxies in greater detail:

NGC 5533.—This large Sab galaxy is the earliest type in the sample. The H I surface densities are rather low, and the distribution in the outer parts is quite patchy. There are also significant side-to-side asymmetries in the outer velocity field, as well as kinematic evidence for a warp (Broeils 1992). Because of this and the low spatial resolution, the galaxy would not have met the BBS criteria. The double-

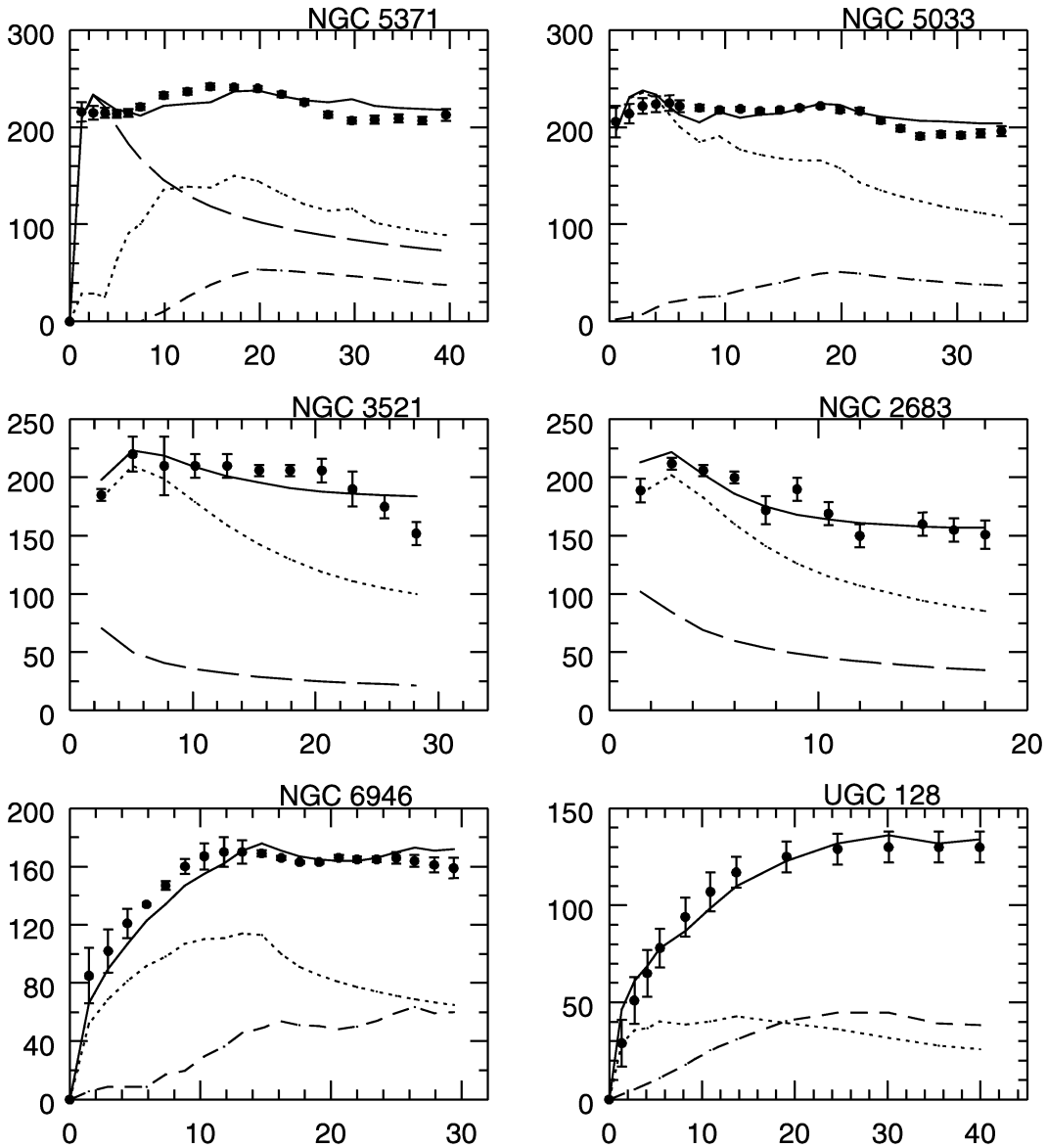

FIG. 1.—*Continued*

exponential bulge-disk decomposition was provided by Y. C. Andredakis (1996, private communication) and implies that a large fraction of the total light is in the bulge. However, the MOND fit to the rotation curve requires that an even larger fraction of the mass be in the bulge. This leads to a bulge M/L of seven and a disk M/L of about one (both in the blue band). While the overall mass-to-light ratio of three in the blue implies that MOND successfully accounts for the magnitude of the discrepancy in this galaxy, near-infrared photometry would be of considerable interest in this case to estimate the distribution of the stellar mass in the central regions.

NGC 6674.—The global blue M/L of 2.6 implies that MOND successfully accounts for the magnitude of the discrepancy; however, the detailed fit is the worst of the sample. The large central rotational velocities and mildly declining rotation curve require a strong central mass concentration. The double-exponential decomposition of the radial light profile by Andredakis does imply that a large fraction of the total luminosity is in the bulge, and this yields reasonable mass-to-light ratios for the bulge and disk. But the real difficulty with the use of this rotation curve is that the galaxy is conspicuously barred (Broeils & Knapen 1991). Moreover, the bar is oriented along the apparent minor axis of the galaxy as projected onto the sky, which, because of elliptical streaming, would have the effect of increasing the apparent rotational velocity in the inner regions. Because of its large-scale nonaxisymmetric structure, this galaxy is clearly not very suitable for detailed rotation-curve modeling.

NGC 5907.—This large, relatively nearby edge-on galaxy has a well-determined and very extended H I rotation curve (Sancisi & van Albada 1987). However, it had not been possible to estimate the Newtonian rotation curve due to the luminous matter, because the high dust obscuration in the plane of the galaxy masks the true radial light distribution. This has changed with the near-infrared photometry of Barnaby & Thronson (1992, 1994), which indicates a more centrally concentrated distribution of luminous material. This highlights the value of near-infrared photo-

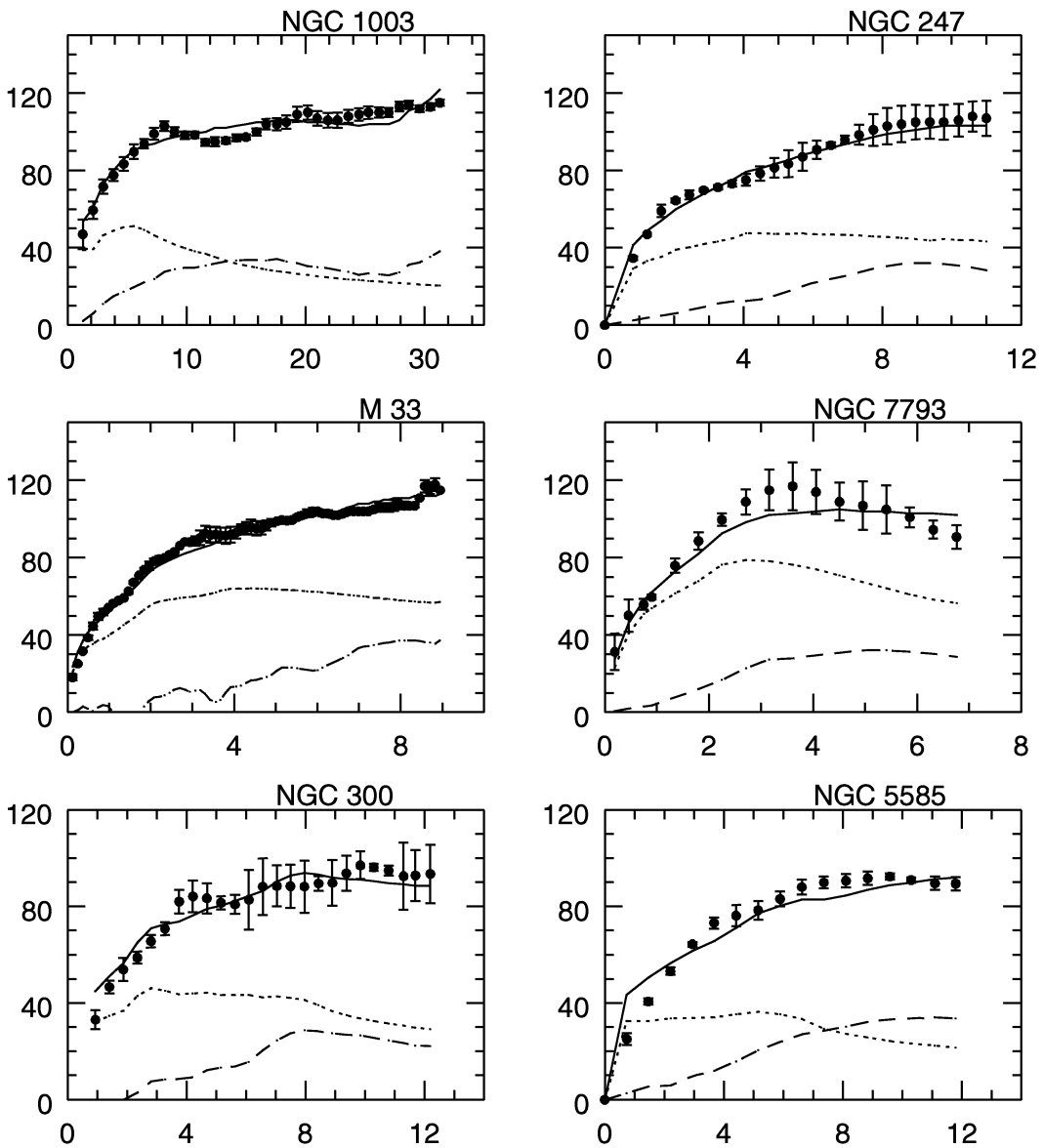

FIG. 1.—*Continued*

metry as the most accurate, absorption-free tracer of the dominant stellar component. Here the decomposition by Barnaby & Thronson into an exponential disk and a bulge represented by a modified Hubble profile is used directly to calculate the Newtonian rotation curve; i.e., because the galaxy is edge-on, the exponential model for the disk is used rather than the detailed photometry.

NGC 3521 and 2683.—These are given by Casertano & van Gorkom (1991) as examples of galaxies with declining rotation curves. The contribution of the gas to the Newtonian rotation curve is not shown here because the mean radial distribution of the gas is not given in this reference; in any case, the total gas mass, estimated from global 21 cm line profiles (Table 1), is less than 10% of the fitted disk mass (Table 3) in both cases. The photometry by Kent (1985) includes decompositions into exponential disks and $r^{1/4}$ law bulges. Here the models, rather than the detailed light distributions, are used to determine the Newtonian rotation curves. The observed rotation curves are not ideal for estimating the true run of circular velocity. In neither case is the rotation curve determined from a full two-dimensional radial velocity field. In NGC 3521, the distribution of H I is asymmetric, extending 20% farther on one side than on the other, and the velocity structure is asymmetric; NGC 2683 is nearly edge-on. Thus these galaxies fail in several respects to satisfy the selection criteria of BBS. Nonetheless, the rotation-curve fits demonstrate that MOND is quite capable of reproducing declining rotation curves if the mass distribution is sufficiently centrally concentrated, a point made by Milgrom in his original paper (Milgrom 1983). In NGC 3521, the abrupt decline in rotational velocity between 20 and 28 kpc could be, if confirmed, problematic for MOND, although it would also be problematic for Newtonian dynamics since the decline is steeper than Keplerian.

UGC 128.—This is a low surface brightness (LSB) spiral galaxy with an extrapolated *B*-band central surface brightness fainter than 23 mag arcsec^{-2} (de Blok et al. 1995). Although it is faint, the linear size is large, with the H I rotation curve extending to 40 kpc. Because the implied

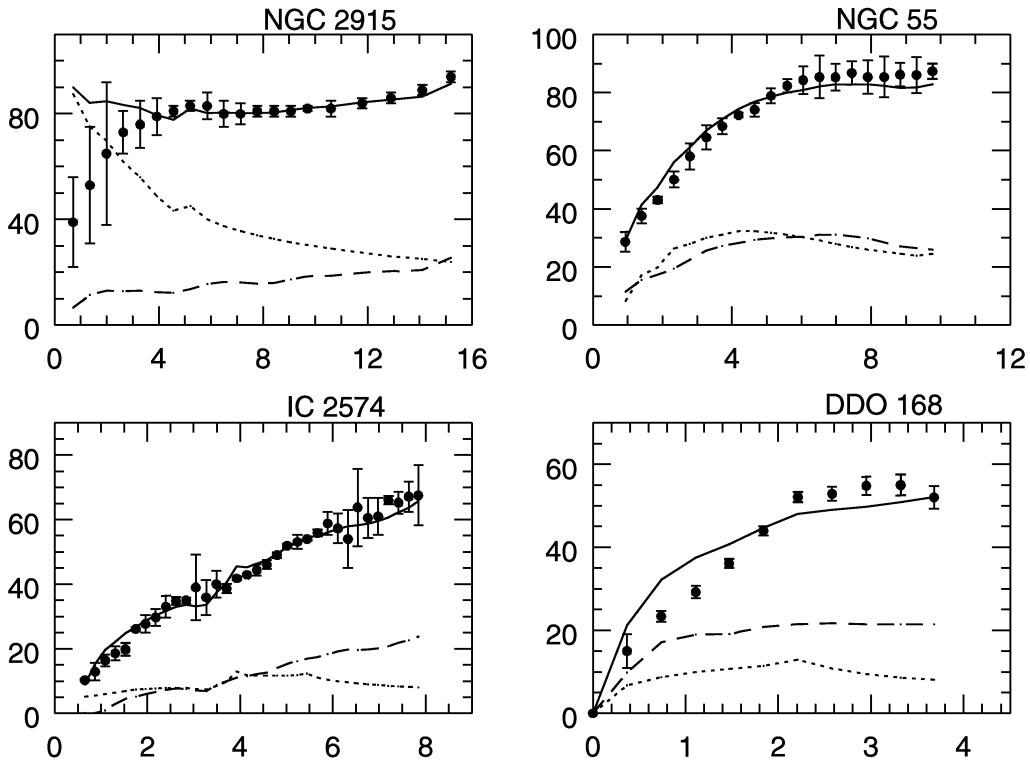

FIG. 1.—*Continued*

surface density is below the MOND critical surface density of a_0/G, the MOND prediction (Milgrom 1983) is that the discrepancy should be large within the optical disk and that the rotation curve should rise slowly to its asymptotic limit. This is seen to be the case, and the MOND rotation curve agrees with the observed curve in detail. It should be emphasized that the general MOND prediction of a large discrepancy in low surface density systems (Milgrom 1983) was made long before observations of systems such as this one confirmed it.

M33.—The observed rotation curve of this classic nearby Sc spiral is from an unpublished analysis by O. M. Kolkman (1995) based upon observations of Deul & van der Hulst (1987; see also Rhee 1996). The large number of independent observed points on the rotation curve, due to the large angular size this object, and the well-established Cepheid distance (Madore & Freedman 1991) make this a good case for detailed rotation-curve fitting, although there is a significant warp in the outer regions.

NGC 2915.—This is a blue compact galaxy (BCG) recently analyzed by Meurer et al. (1996). The neutral hydrogen extends well beyond the bright optical image (to 22 times the exponential scale length), and the observed rotation curve remains constant, with a suggestion of a rise at the outermost measured points. This implies a very large discrepancy between the visible and Newtonian dynamical mass (hence the authors refer to this object as the darkest disk galaxy). The MOND rotation curve is higher than the observed curve in the inner regions (where the errors are large) but agrees very well with the observed rotation curve in the outer regions. Here even the apparent rise of rotational velocity in the last few points is reproduced, as a result of the contribution of the gas to the dynamical mass. However, in spite of this agreement, the implied mass–to–blue light ratio for the disk is 6.9, which is an uncomfortably large value for a BCG. The distance to the galaxy is quite uncertain; Meurer et al. gave 5.3 ± 1.3 Mpc based on the method of brightest stars. At a distance of 6.6 Mpc, M/L is reduced to 3.3. It might also be that the luminosity has been underestimated if a faint luminous halo surrounds the bright, blue compact object.

DDO 168.—This is a dwarf with a small bar in the central regions. The MOND rotation curve lies noticeably above the observed rotation curve in the inner regions. This should not be given too much significance, because of the possible effects of the bar or of beam smearing.

Table 3 lists the fitted disk and bulge masses for all galaxies in the present sample, as well as those in the sample of BBS—a total of 33 galaxies for which MOND rotation curves have been calculated. Also shown are the implied mass–to–blue light ratios, for the disk and bulge separately where applicable. In column (6), the global (bulge plus disk) mass-to-light ratio in the blue is given for the luminous (stellar) component, M^*/L_B; in column (7), the ratio of the total mass (stars plus gas) to luminosity in the blue band is given (M_t/L_B); in column (8), the ratio of the total mass to luminosity in the H band (M_t/L_H) is given for those galaxies for which an H-band magnitude has been measured. It should be noted that the fitted mass, M^*, includes not only the mass in luminous stars but also any other component that is distributed like the stars, such as, possibly, the molecular gas.

We see that in most cases the global mass-to-light ratios are reasonable and consistent with population synthesis models; i.e., the models imply blue-band M/L-values in the range from a few tenths to 10, depending upon the star formation history and metallicities (Bruzual & Charlot

1993; Worthy 1994). More importantly, there are no very high values (the highest being for NGC 2915, discussed above), which means that MOND can certainly account for the magnitude of the global mass discrepancy, i.e., there is no suggestion that additional unseen matter is needed. Although there are several very low values of M^*/L_B (see below), none of the fitted masses are negative (this is possible, considering that the gas mass is measured directly), i.e., in no case does MOND seriously overcorrect for the discrepancy.

5. GLOBAL MASS-TO-LIGHT RATIOS AND THE TULLY-FISHER RELATION

Figure 2 shows the global blue stellar mass-to-light ratios (M^*/L_B) of the sample galaxies determined from the MOND fits (col. [6] of Table 3) plotted as a function of asymptotic rotational velocity. There is a range of a factor of almost 100, but there is also an apparent trend of increasing M^*/L_B with increasing rotational velocity. Because of the sensitivity of the blue luminosity to star formation activity, this would be consistent with more active star formation in the lower luminosity gas-rich galaxies in this sample. But the overall consistency of the implied M^*/L_B-values with population synthesis models is demonstrated by Figure 3. This is a plot of the MOND M^*/L_B versus $B-V$ color for those galaxies in the sample with a reddening-corrected $B-V$ listed in the Third Reference Catalogue (de Vaucouleurs et al. 1991). Also shown is M/L_B as a function of $B-V$ predicted from the population synthesis models of Larsen & Tinsley (1978); here the properties are those of a population of stars evolved for 10^{10} yr with various prescriptions for a monotonically decreasing star formation rate. It is seen that the general trend of decreasing M/L with increasing blueness is present in the MOND values of M^*/L_B.

There are, however, five galaxies in Figure 3 with implied values of M^*/L_B less than 0.25: NGC 55, DDO 168, NGC 1003, IC 2574, and DDO 154. While such low mass-to-light ratios are possible in extreme starburst galaxies, it should be noted that all of these objects are nearby (<4 Mpc) gas-rich dwarfs. For such objects, the implied M^*/L-values are extremely sensitive to the adopted distance. For example, for NGC 3109 (not plotted here), the distance used by BBS is a Cepheid-based estimate of 1.7 Mpc (Sandage & Carlson 1988). At this distance, the measured mass of gas is almost 100% of the MOND mass (eq. [4]), which means that $M^*/L_B \approx 0$. A more recent Cepheid distance estimate is 1.3 Mpc (Capaccioli, Piotto, & Bresolin 1992). At this distance, the gas mass is reduced to ~60% of the MOND mass, which means that M^*/L_B is increased to 0.6. So, given the distance uncertainties in these gas-rich dwarfs, it is not surprising that some of the fitted values of the stellar M/L would be unrealistic; the point is that M^*/L_B is the single fitted parameter and must reflect all uncertainties involved in this procedure.

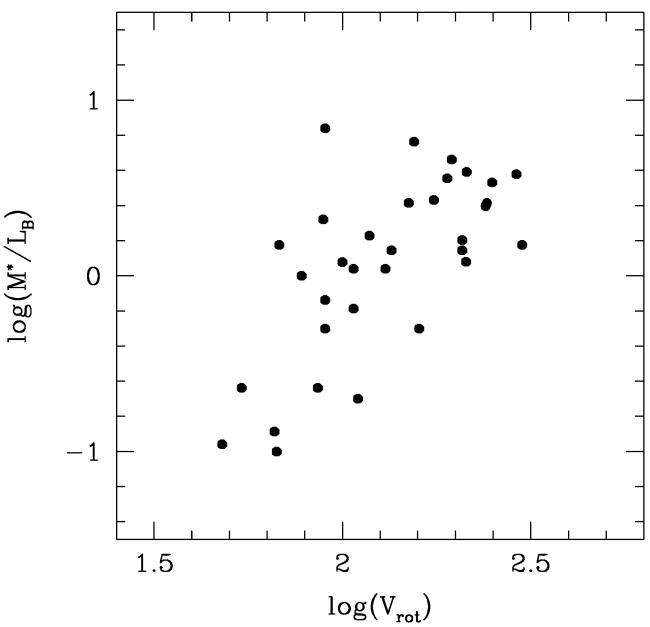

FIG. 2.—A log-log plot of M^*/L_B vs. the observed asymptotic rotational velocity for the sample galaxies. Here M^* is the total mass of the stellar component (disk plus bulge) determined from the MOND fit.

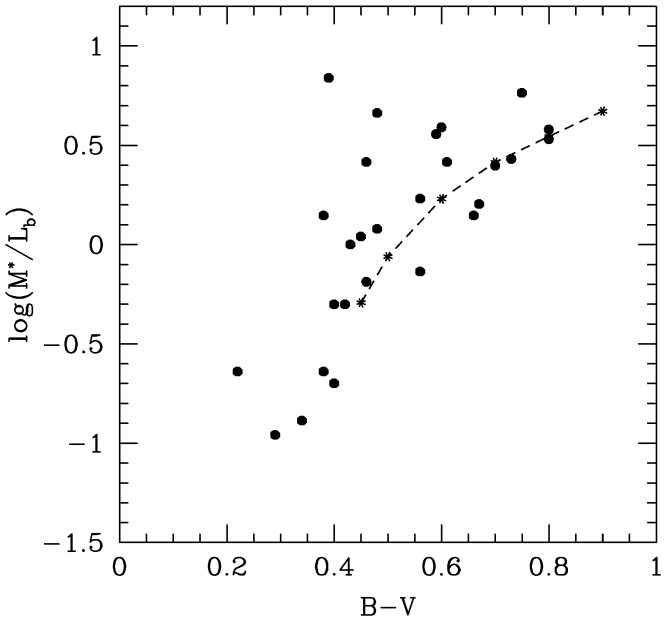

FIG. 3.—Logarithm of M^*/L_B of sample galaxies vs. the reddening-corrected $B-V$ color from de Vaucouleurs et al. (1991). Also shown (*dashed line*) are theoretical M/L_B from the population synthesis models of Larson & Tinsley (1978).

Figures 4 and 5 show the observed B- and H-band luminosity–rotational velocity relationships (Tully-Fisher) for the galaxies in the combined total sample (Table 3). Here the rotational velocity is that measured at the most distant points for which the determination is reliable; this would correspond most closely to the asymptotic circular velocity in the context of MOND (eq. [4]). The H-band relation is plotted for those 15 galaxies in the combined sample with measured H-band magnitudes (Tormen & Burstein 1995). In both cases, the relation appears quite linear on the log-log plot, with a slope near the canonical value of four. The slopes are somewhat larger (4.0 ± 0.25 in the blue, 4.4 ± 0.19 in the near-infrared) than usually encountered, primarily because the use of the actual rotation curve yields a larger value of the rotational velocity for the low-luminosity galaxies than does the global 21 cm line profile. The scatter in log luminosity is 0.30 in the blue, corresponding to 0.75 mag. In the near-infrared the correlation is much tighter (as is well known), with a scatter of 0.12 (0.3 mag). The tightness of the relation implies that the errors in distance (at least for this subsample of 15) are not large.

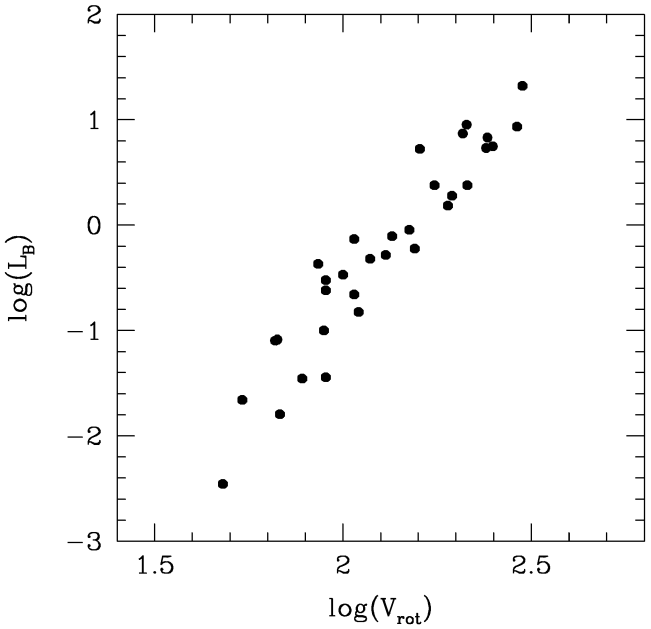

FIG. 4.—A log-log plot of the *B*-band luminosity of the sample galaxies in units of 10^{10} $L_\odot$ vs. the observed asymptotic rotational velocity (the *B*-band Tully-Fisher relation).

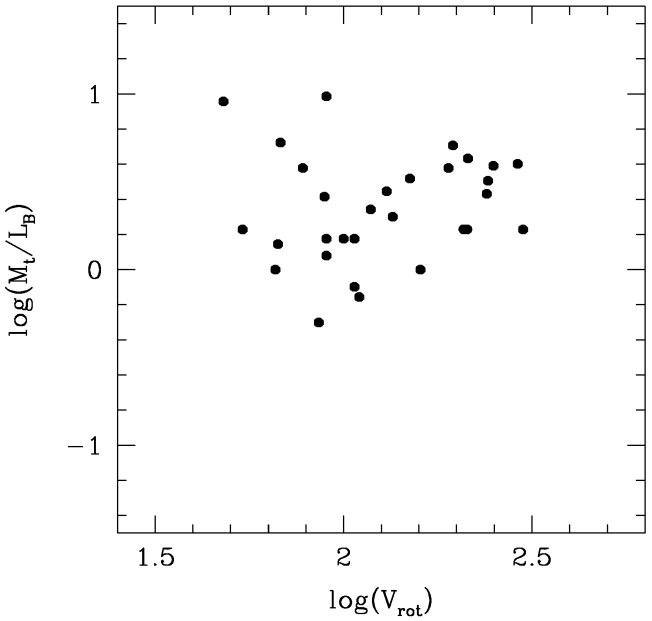

FIG. 6.—A log-log plot of M_t/L_B vs. the observed asymptotic rotational velocity. Here $M_t = M^* + M_g$. This is the total mass of the galaxy—the mass of the stellar component determined from the MOND fit plus M_g, the mass of the gaseous component.

In the context of MOND, there is a total mass–asymptotic rotational velocity relation that is *exact* (eq. [4]). There is a similar luminosity-velocity relation only for a luminosity indicator that is proportional to the mass, i.e.,

$$v^4 = Ga_0(M_t/L)L \ . \qquad (5)$$

Therefore the scatter in the observed relation, apart from observational errors (e.g., inaccuracies in the rotational velocity or the global magnitude, errors in the distance), would only be due to intrinsic scatter in the mass-to-light ratio. The tightness of the observed relation suggests that this might, in fact, be small.

However, as we see in equation (5), it is not the mass-to-light ratio of the luminous matter, M^*/L, that is relevant to the slope and scatter in the observed Tully-Fisher (TF) relation but rather the *total mass*–to–light ratio (M_t/L). The gas mass can make a very significant contribution to this total in low-mass, low-luminosity galaxies. In Figure 6, we see the total mass–to–blue light ratio (col. [7] of Table 3) plotted against the asymptotic rotational velocity, where now the

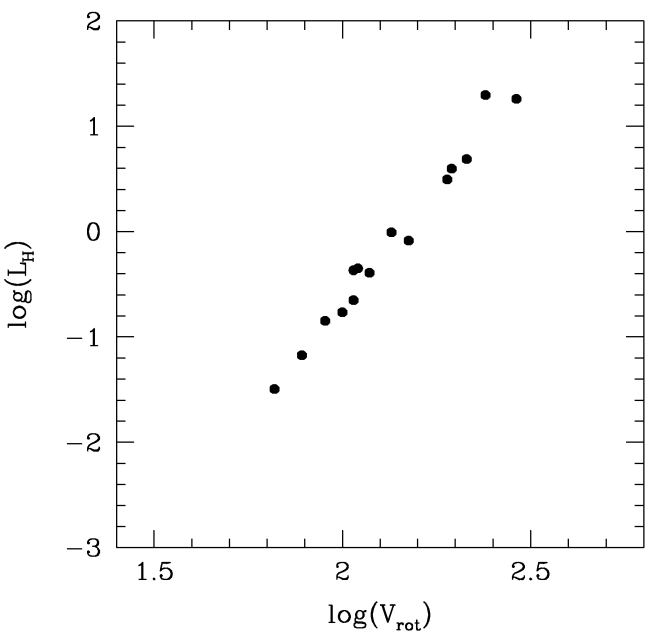

FIG. 5.—A log-log plot of the *H*-band luminosity (10^{10} $L_\odot$) vs. the observed asymptotic rotational velocity (the *H*-band Tully-Fisher relation). Only 15 galaxies from our sample have measured *H*-band magnitudes.

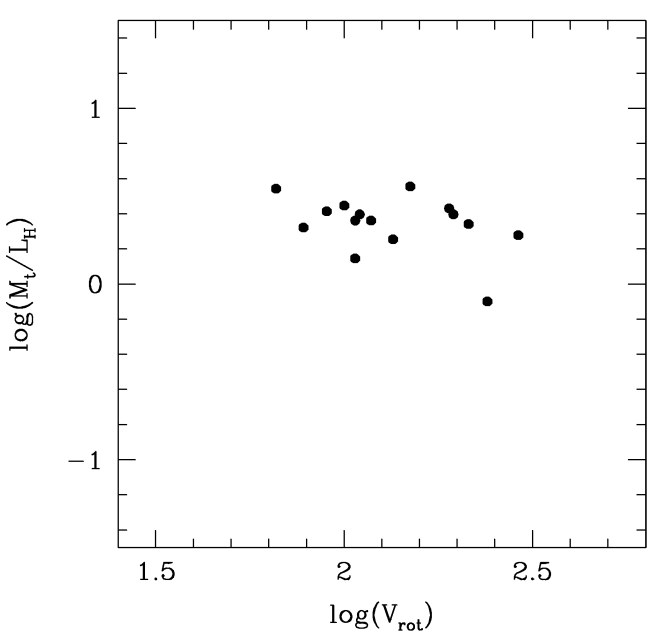

FIG. 7.—A log-log plot of M_t/L_H vs. observed asymptotic rotational velocity for those 15 sample galaxies with measured *H*-band magnitudes. The scatter in this measured M/L is comparable to the scatter in the observed *H*-band Tully-Fisher relation.

total mass includes the observed neutral hydrogen plus implied helium mass. The range in this quantity is about a factor of 15, and the mean value is 1.9 with a dispersion of 1.7; that is, the scatter is now ~90%, which is quite consistent with the 97% scatter observed in the blue TF relation (Fig. 4). It is also evident that, for a number of the low-luminosity dwarf galaxies, the total mass–to–light ratio is quite large, opposite to the trend noted in Figure 2. This is entirely due to the large contribution of the (nonluminous) gas to the total mass in these systems. This increase in actual mass-to-light ratio can result in a steepening of the observed TF law at low luminosities—a steepening that has previously been noted in much larger samples (Aaronson et al. 1982).

In Figure 7, we see the total mass–to–light ratio in the near-infrared (col. [8] of Table 3) plotted against rotational velocity. Here the range in M/L is reduced to about a factor of 2; the mean value is 2.3, with a dispersion of 0.73. This scatter of 31% is again entirely consistent with the scatter of 33% in the observed infrared TF law (Fig. 5). There is also a slight trend of increasing M_t/L with decreasing rotational velocity. This, again, is due to the increasing contribution of the gas mass in the lower luminosity systems and would be consistent with a slope somewhat larger than four in the observed TF relation.

6. IS A DEFINITIVE FALSIFICATION POSSIBLE?

The one-parameter MOND rotation curve fits to the galaxies in the highly selected sample of BBS are, with one exception, in very precise agreement with the observed rotation curves. In the larger sample considered here, a number of the rotation curves are not perfectly fitted; one can argue that this is because of the various uncertainties mentioned (distance errors, beam smearing, warps, noncircular motions, contribution of molecular gas, imprecise bulge-disk decomposition, the use of visual rather than infrared magnitudes to trace the stellar density distribution, true radial variations in M/L of the stellar population). Nonetheless, the overall form of the rotation curves and general trend with luminosity are generally quite well reproduced, with the MOND rotation curves of luminous, high surface brightness galaxies exhibiting the rapid rise and then decline to an asymptotic value and those of the low-luminosity, low surface brightness galaxies rising slowly to the asymptotic value as is observed. But, because of the unknown systematic effects, which may give rise to a difference between the measured rotation curve and the true run of circular velocity, it is not useful to apply a statistical goodness-of-fit criterion to assess objectively the success of MOND in reproducing observed rotation curves from the distribution of detectable matter.

Then the question naturally arises what would constitute a bad MOND rotation curve fit. Is it in fact possible to definitively falsify MOND by this technique? Can an example be given in which MOND fundamentally fails to predict the observed rotation curve of a spiral galaxy? There is such a case, and this is the exceptionally bad fit to NGC 2841 in the sample of BBS if this galaxy is at its Hubble law distance of 9.5 Mpc ($h = 0.75$). This MOND rotation curve fit to NGC 2841 is reproduced in Figure 8*a*. Not only is the rotation curve badly fitted, but the implied bulge and disk mass-to-light ratios are outrageous: $(M/L)_b = 0.6$ and $(M/L)_d = 13$. The basic problem is that the form of the observed rotation curve, compared to the Newtonian rotation curve of the detectable matter, suggests that a large discrepancy is present at accelerations larger than a_0, which is not possible in the context of MOND. The data upon which the measured rotation curve is based are of the highest quality in the existing literature (Begeman 1987): there is sufficient spatial resolution; the H I distribution is reasonably smooth and symmetric; the outer warp evident in the gas kinematics is symmetric and well modeled by the tilted-ring algorithm. Only a large and improbable positive radial gradient in M/L in the disk itself could allow this rotation curve to be explained by MOND, using the standard value of a_0.

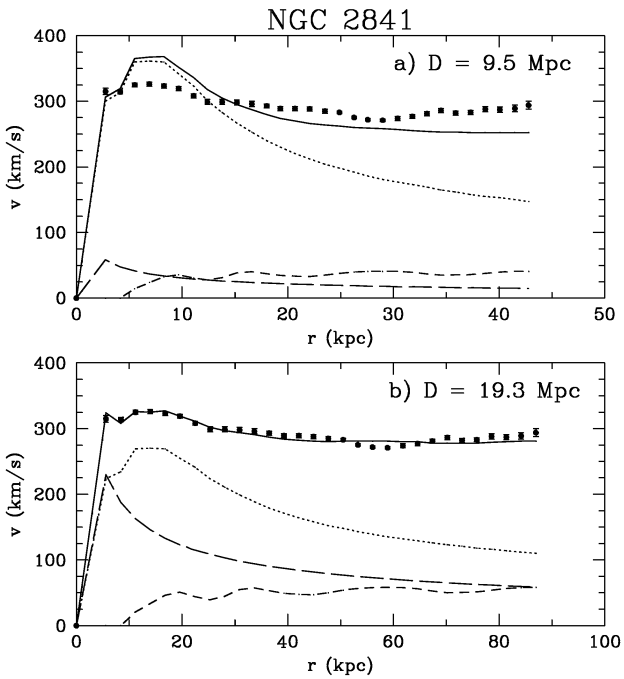

FIG. 8.—(*a*) MOND fit to the rotation curve of NGC 2841, assuming that this galaxy is at its Hubble law distance ($H_0 = 75$ km s^{-1} Mpc^{-1}) of 9.5 Mpc. The Newtonian rotation curves of the various components are shown as in Fig. 1. This is an example of an unacceptable MOND fit. The fitted bulge and disk mass-to-light ratios in the blue are 0.6 and 13, respectively. (*b*) MOND fit to the rotation curve of NGC 2841, allowing distance to be a free parameter. The implied distance, 19.3 Mpc, is twice the Hubble law distance. Here the bulge and disk M/L-values are 4.3 and 3.5, respectively.

BBS noted that if the distance is allowed to be a parameter in the least-squares fit, MOND fits for most of their sample improve slightly; the fitted distance agrees well with the Tully-Fisher distance and is generally within 15% of the Hubble law distance. The one exception is the case of NGC 2841, which requires a distance twice as large as the Hubble law distance to achieve a reasonable MOND fit; i.e., 19.3 rather than 9.5 Mpc (the luminosities and M/L-values for this object given in Table 3 are based upon this larger distance). The MOND rotation curve fit to this galaxy at the larger distance is shown in Figure 8*b*. Here the fitted curve agrees well with the observed curve, and the implied M/L-values are much more reasonable: 3.5 for the disk and 4.3 for the bulge (based upon a new double-exponential decomposition by Y. C. Andredakis). NGC 2841 is the only galaxy out of the total sample of 33 that requires a distance substantially different than the Hubble law distance in order to achieve a reasonable MOND fit to the rotation curve. This larger distance is consistent with all Tully-

Fisher determinations; for example, Aaronson & Mould (1983) gave a distance of 15.6 Mpc to the NGC 2841 group based upon the H-band Tully-Fisher relation. But in fact, Tully-Fisher distances are not independent of the fitted MOND distance, because MOND subsumes the Tully-Fisher relation (eq. [5]). Thus a truly independent and reliable distance estimate for this galaxy (e.g., Cepheids) offers the possibility of a definitive falsification of MOND: if the galaxy is close to its Hubble law distance, the viability of MOND is seriously threatened (one well-established counterexample is sufficient); if the galaxy is twice as far away as the Hubble law distance, MOND remains viable.

Given the existence of large-scale flows, it is not surprising that one galaxy out of 33 might have a distance significantly different from that implied by uniform Hubble flow; however, there is a Hubble law, and it would be quite negative for MOND if distances to several galaxies in the sample had to be adjusted by such a large factor to achieve reasonable fits.

7. CONCLUSIONS

The 22 galaxies considered here along with the 11 galaxies previously considered by BBS constitute the current total published sample of galaxies (plus or minus two or three) with optical or infrared surface photometry and with observed H I rotation curves extending well beyond the optical image of the galaxy. Although this number will rapidly grow as a consequence of several large surveys now underway, this sample of 33 galaxies constitutes, at present, the entire body of data relevant to the nature of the discrepancy between the classical dynamical and visible mass in galaxies (the several hundred optical rotation curves in the literature do not, in general, extend far enough to probe the systematics of the discrepancy). BBS considered a highly selected subsample of this collection of rotation curves—galaxies for which one can be reasonably sure that the measured 21 cm line rotation curve provides a fairly good estimate of the run of circular velocity and, thus, the radial force beyond the optical image. They demonstrated that the observed distribution of detectable matter in the galaxies, in the context of MOND, reproduced the observed rotation curves quite accurately, often down to rather small details, without invoking unseen matter.

Here the remainder of the current total sample of these galaxies, i.e., objects that either do not meet the selection criteria of BBS or those added since 1991, have been considered in the context of MOND. Compared to the BBS sample, some deterioration in the quality of the fits is expected and seen, but in general, the form and amplitude of the observed rotation curves are also reproduced for these additional galaxies. The reader, when assessing the quality of the fits in Figure 1, should keep in mind that, unlike the usual dark halo models, there are only one or, in some cases, two adjustable parameters per galaxy, and these are the mass of the luminous components. The MOND acceleration parameter has been fixed at the BBS value of 1.2×10^{-8} cm s^{-2} (normalized to the distance scale of $H_0 = 75$ km s^{-1} Mpc), and the distance to each galaxy has been fixed at its value determined via the Hubble law or by more direct methods (in particular, Tully-Fisher distances have not been used since these are, in effect, the MOND distances).

For the large luminous galaxies with central bulges or light concentrations, such as NGC 5533 and 801, the MOND fits require a mass distribution that is even more centrally concentrated than the light distribution. This implies (see Table 3) a bulge M/L that is significantly larger than the disk M/L, but the exact values depend quite critically upon how the light distribution is decomposed into bulge and disk contributions. Because of this complication of bulge-disk decomposition and the possibility of an extra free parameter, these systems, with respect to rotation-curve analysis, are not as clean as pure disk galaxies. But in general a higher bulge M/L would be more consistent with expectations for possibly older, or at least less actively star forming, spheroidal subsystems. It is significant that, for those galaxies without a conspicuous bulge, MOND does not require, in any single case, a larger central M/L in order to achieve a reasonable fit to the rotation curve; that is, the necessity of a larger central M/L occurs only in those cases in which the obvious presence of a separate bulge component justifies it.

MOND does quite well in reproducing the rotation curves of the pure disk systems (e.g., M33); in particular, the scheme works well for the low surface brightness galaxy UGC 128 and for the gas-rich systems such as NGC 2915, NGC 55, and IC 2574. This not only lends support to MOND but also to the assumptions that underlie the whole procedure, such as constancy of the mass-to-light ratio within the disk component of any given galaxy and the absence of a significant contribution to the detectable mass by molecular gas with a radial density distribution that differs from that of the luminous disk.

When assessing the quality of MOND or dark halo fits to galactic rotation curves, one should also consider the physical plausibility of the fitted parameter or parameters. In this work, if we neglect the ambiguous procedure of bulge-disk decomposition, the only parameter to consider is the global stellar mass-to-light ratio. We have noted above that the implied global M^*/L_B-values, although spanning a range from 0.1 to 7, are not so high as to require substantial additional dark matter, which would be contrary to the spirit of MOND, nor are there negative values, which would suggest that MOND substantially overcorrects (a number of negative stellar mass-to-light ratios would constitute a falsification of the theory). Moreover, the range in this one fitted parameter must reflect all of the uncertainties of the procedure, e.g., distance errors, noncircular motion, and the use of visual photometry. Even so, the fitted values of M^*/L in the blue and H bands are generally consistent with those implied by stellar population models and exhibit the trend of increasing M^*/L_B with redder color.

When the ratio of total mass (the fitted luminous mass plus measured gas mass) to light is considered, the scatter is reduced considerably and becomes quite consistent with the observed scatter in the blue Tully-Fisher relation. This is even more striking in the near-infrared, where the scatter in the total mass–to–light ratio is reduced to the order of 30%, which again is comparable to the scatter in the near-infrared Tully-Fisher relation. Not all of this scatter is intrinsic; some of the apparent scatter in M_t/L certainly results from errors in the estimated distances (in MOND, the total mass estimate is fairly independent of distance, implying that M_t/L scales as the inverse square of the distance). With this in mind, the overall small scatter in the implied M_t/L-values, where M_t includes the fitted MOND mass for the luminous component, argues forcefully for the plausibility of the implied MOND masses.

For the combined sample of 33 galaxies, MOND fails only in one case: the MOND fit to the well-determined rotation curve of NGC 2841 is not acceptable. The failure is serious; not only is the form of the observed rotation curve not reproduced, but implied mass-to-light ratios of the bulge and disk are implausible (the implied disk M/L of 13 means that MOND fails to account for the magnitude of the discrepancy). If, however, NGC 2841 is at twice the distance implied by the Hubble law, the predicted MOND curve agrees with the observed curve in detail and the implied M/L-values are reasonable. An independent distance determination to this galaxy (i.e., independent of the Tully-Fisher relation) is therefore crucial for MOND; a distance significantly less than 19 Mpc would falsify the idea.

In general, the analysis of this larger sample reinforces the conclusions of BBS: in terms of the number of parameters, MOND provides the most efficient description of the systematics of galactic rotation curves. Given the observed distribution of light and gas in a galaxy, one may predict with considerable precision the extended rotation curve that is actually observed by adjusting only the M/L of the luminous component, and this required M/L (in the near-infrared at least) lies within a rather small range around a mean value of approximately two in solar units. But it is not just that MOND requires a smaller number of parameters to describe rotation curves than do dark halo models. The philosophy of rotation-curve fitting is really quite different for the two hypotheses: dark matter rotation curves are fits that define the properties of the dark halo; MOND rotation curves are predictions that test the validity of the theory. MOND is a viable alternative to the dark matter hypothesis precisely because of its predictive successes.

Because of surveys presently underway, there will soon be a rapid increase in the number of high-quality rotation curves in the literature. In the context of the "missing mass problem," it will be of great interest to assess the continued performance of MOND in predicting the rotation curves for a larger number of spiral galaxies with a wider range of properties.

I am very grateful to a number of people for either sharing their data with me in advance of publication or for providing existing data in convenient form. These include H. Hoekstra, M.-H. Rhee, E. de Blok, R. Sancisi, and A. Broeils. In particular, Adrick Broeils has done this analysis for a number of these galaxies observed as part of his Ph.D. dissertation, and he has recently confirmed several of the cases shown here. I thank G. R. Meurer and C. Carignan for data in advance of publication and for very useful comments on their observations of the blue compact galaxy NGC 2915. I thank Y. C. Andredakis for his careful bulge-disk decompositions. As always, when it comes to analysis of rotation curves, the advice and help of K. G. Begeman is invaluable. I thank him especially for initiating me into the wonders of GIPSY. Finally, I am most grateful to M. Milgrom. His comments and insight have been, as always, an enormous help and encouragement in this work.

REFERENCES

Aaronson, M., & Mould, J. 1983, ApJ, 265, 1
Aaronson, M., et al. 1982, ApJS, 50, 241
Andredakis, Y. C., & Sanders, R. H. 1994, MNRAS, 267, 283
Barnaby, D., & Thronson, H. A., Jr. 1992, AJ, 103, 41
———. 1994, AJ, 107, 1717
Begeman, K. G. 1987, Ph.D. thesis, Univ. Groningen
Begeman, K. G., Broeils, A. H., & Sanders, R. H. 1991, MNRAS, 249, 523 (BBS)
Bekenstein, J. D., & Milgrom, M. 1984, ApJ, 286, 7
Brada, R., & Milgrom, M. 1995, MNRAS, 276, 453
Broeils, A. H. 1992, Ph.D. thesis, Univ. Groningen
Broeils, A. H., & Knapen, J. H. 1991, A&AS, 91, 469
Bruzual A., G., & Charlot, S. 1993, ApJ, 405, 538
Capaccioli, M., Piotto, G., & Bresolin, F. 1992, AJ, 103, 1151
Carignan, C. 1985, ApJS, 58, 107
Carignan, C., Charbonneau, P., Boulanger, F., & Viallefond, F. 1990, A&A, 234, 43
Carignan, C., & Puche, D. 1990a, AJ, 100, 394
———. 1990b, AJ, 100, 641
Casertano, S., & van Gorkom, J. H. 1991, AJ, 101, 1231
Coté, S., Carignan, C., & Sancisi, R. 1991, AJ, 102, 904
de Blok, W. J. G., van der Hulst, J. M., & Bothun, G. D. 1995, MNRAS, 274, 235
Deul, E. R., & van der Hulst, J. M. 1987, A&AS, 67, 509
de Vaucouleurs, G. H., de Vaucouleurs, A., Corwin, H. G., Buta, R., Paturel, G., & Fouqué, P. 1991, Third Reference Catalogue of Bright Galaxies (New York: Springer)
Freedman, W. L., Madore, B. F., Hawley, S. L., Horowitz, I. K., Mould, J., Navarrete, M., & Sallmen, S. 1992, ApJ, 396, 80
Kent, S. M. 1984, ApJS, 56, 105
———. 1985, ApJS, 59, 115
Kent, S. M. 1986, AJ, 91, 1301
———. 1987, AJ, 93, 806
Kraan-Korteweg, R. C. 1986, A&AS, 66, 255
Larson, R. B., & Tinsley, B. M. 1978, ApJ, 219, 46
Madore, B. F., & Freedman, W. L. 1991, PASP, 103, 933
Martimbeau, N., & Carignan, C. 1994, AJ, 107, 543
Meurer, G. R., Carignan, C., Beaulieu, S. F., & Freeman, K. C. 1996, AJ, 111, 1551
Meurer, G. R., Mackie, G., & Carignan, C. 1994, AJ, 107, 2021
Milgrom, M. 1983, ApJ, 270, 365
———. 1986, ApJ, 302, 617
———. 1988, ApJ, 333, 684
———. 1994, Ann. Phys., 229, 384
Puche, D., Carignan, C., & Wainscoat, R. J. 1991, AJ, 101, 447
Rhee, M.-H. 1996, Ph.D. thesis, Univ. Groningen
Roelfsema, P. R., & Allen, R. J. 1985, A&A, 146, 213
Rubin, V. C., Burstein, D., Ford, W. K., Jr., & Thonnard, N. 1985, ApJ, 289, 81
Sancisi, R., & van Albada, T. S. 1987, in IAU Symp. 117, Dark Matter in the Universe, ed. J. Kormendy & G. R. Knapp (Dordrecht: Reidel), 67
Sandage, A., & Carlson, G. 1988, AJ, 96, 1599
Sanders, R. H. 1990, A&A Rev., 2, 1
Sanders, R. H., & Begeman, K. G. 1994, MNRAS, 266, 360
Tormen, G., & Burstein, D. 1995, ApJS, 96, 123
van der Hulst, J. M., Skillman, E. D., Smith, T. R., Bothun, G. D., McGaugh, S. S., & de Blok, W. J. G. 1993, AJ, 106, 548
Wevers, B. M. H. R. 1984, Ph.D. thesis, Univ. Groningen
Worthy, G. 1994, ApJS, 95, 107
Young, J. S. 1987, in IAU Symp. 115, Star Forming Regions, ed. M. Peimbert & J. Jugaku (Dordrecht: Reidel), 557